

# Microscopic theory of the current-voltage characteristics of Josephson tunnel junctions

Sang-Jun Choi<sup>1,\*</sup> and Björn Trauzettel<sup>1,2</sup>

<sup>1</sup>*Institute for Theoretical Physics and Astrophysics,  
University of Würzburg, D-97074 Würzburg, Germany*

<sup>2</sup>*Würzburg-Dresden Cluster of Excellence ct.qmat, Germany  
(Dated: December 21, 2021)*

Deep theoretical understanding of the electrical response of Josephson junctions is indispensable regarding both recent discoveries of new kinds of superconductivity and technological advances such as superconducting quantum computers. Here, we study the microscopic theory of the DC current-biased  $I$ - $V$  characteristics of Josephson tunnel junctions. We derive an analytical formula of the  $I$ - $V$  characteristics of generic junctions. We identify subharmonics of the  $I$ - $V$  characteristics and their underlying mechanism as the feedback effect of intrinsic AC currents generated by voltage pulses in the past. We apply our theory to analytically solve the Werthamer equation and describe various DC current-biased  $I$ - $V$  characteristics as a function of softening of the superconducting gap. Strikingly, we identify voltage staircases of the  $I$ - $V$  characteristics in a genuine Josephson junction without AC current bias or qubit dynamics. Our general analytical formalism opens new avenues for a microscopic understanding of  $I$ - $V$  characteristics of Josephson junctions that have been limited to phenomenological models so far.

Microscopic theories of Josephson tunnel junctions were established at the early stages of the discovery of the Josephson effect [1–5]. For the DC voltage-biased junctions yielding intriguing phenomena such as multiple Andreev reflections [2, 6–10], the  $I$ - $V$  characteristics can be well understood with the simple equation of motion of the superconducting phase difference  $\phi(t)$  with  $\dot{\phi}(t) = 2eV/\hbar$  at voltage bias  $V$ . However, DC current-biased junctions are governed by a nonlinear and nonlocal-in-time integro-differential equation, and a microscopic theory of the DC current-biased  $I$ - $V$  characteristics of Josephson junctions requires to solve the complex dynamics of  $\phi(t)$ .

While the  $I$ - $V$  characteristics of DC current-biased Josephson junctions are widely examined experimentally, its theoretical analysis has been limited to phenomenological theories [11–14], adiabatic approximations [5, 14], or numerical approaches [15–17], in which several drawbacks are faced. The analytical theories on the  $I$ - $V$  characteristics are typically based on reducing the nonlocal-in-time integro-differential governing equation of  $\phi(t)$  into a local-in-time differential equation. However, those theories, especially at low temperature, are self-consistent only for zero voltage  $V = 0$  or in the Ohmic regime  $V \gg I_c R_n$ . The inconsistency of the analytical theories at intermediate voltages,  $0 < V < I_c R_n$ , is related to the fast dynamics of  $\phi(t)$  resulting in voltage pulses [18]. These voltage pulses are inevitable due to the nonlinear nature of the supercurrent [19]. While numerical approaches have been successfully implemented in the frequency-domain, they have mainly been performed for conventional BCS superconductors. Thus, it is imperative to put forward a rigorous analytical theory, which is consistent and generally applicable to various types of current-biased Josephson junctions.

In this Letter, we study the microscopic theory of DC current-biased  $I$ - $V$  characteristics of generic Josephson

tunnel junctions. The gist of our approach is to analyze the general behavior of the superconducting phase  $\phi(t)$  generated by successive voltage pulses in the time domain. With this approach, we show that the voltage pulses dynamically modulate the tilted washboard potential in the RSJ model. This viewpoint provides us with a clear understanding of the complex dynamics of  $\phi(t)$ . Focusing on an intermediate voltage strength across the junction, we find that the retarded response of the Josephson junctions is decisive for the  $I$ - $V$  characteristics. This enables us to obtain an analytical formula of the  $I$ - $V$  characteristics for general memory kernels in arbitrary Josephson tunnel junctions.

We apply our theory to the seminal example of the Werthamer equation including smearing of the quasiparticle density of states (DOS). We emphasize the validity of our approach by a convincing agreement between numerics and our analytical formula. If the smearing is small, we predict voltage staircases in DC current-biased  $I$ - $V$  characteristics resembling Shapiro steps that occur if an additional AC current bias is applied to the junction. Finally, we show that a substantial smearing of the DOS can justify the validity of the RSJ model at zero temperature but with hystereses due to nonequilibrium Josephson effects. Both voltage staircases and hystereses are experimentally observed in high-quality Josephson junctions [20–24]. In the presence of a qubit formed in the junction, voltage staircases and hystereses have recently been predicted in the DC current-biased case as well [25–27]. In a genuine Josephson junction, this effect is not yet understood but explained by us below.

*Dynamical washboard potential model.*— The microscopic theory of Josephson tunnel junctions was established within the tunneling Hamiltonian formalism [1–3] and developed to relate current and voltage across the junction to an arbitrary superconducting phase differ-

ence  $\phi(t)$  [4, 5]. For a DC current bias  $I$ , the dynamics of  $\phi(t)$  follows the nonlinear integro-differential equation,

$$I = \frac{\hbar}{2eR_n} \frac{d\phi}{dt} + \int_{-\infty}^t dt' \mathcal{K}_n(t-t') \sin \frac{\phi(t) - \phi(t')}{2} + \int_{-\infty}^t dt' \mathcal{K}_s(t-t') \sin \frac{\phi(t) + \phi(t')}{2}. \quad (1)$$

The first term on the right hand side is the instantaneous Ohmic response of the quasiparticle current. The second term is the retarded response of the quasiparticle current. The third term is the retarded response of the supercurrent. The retarded responses stem from the frequency-dependent tunneling currents caused by the particular gap structures of given superconducting electrodes [28, 29]. Memory kernels  $\mathcal{K}_{n,s}(t)$  describe retarded responses by coupling the past dynamics of  $\phi(t')$  at  $t'$  to  $\phi(t)$  at the present time  $t > t'$ . The dynamics of  $\phi(t)$  determines the DC voltage drop  $V \equiv \lim_{\tau \rightarrow \infty} \frac{1}{\tau} \int_0^\tau dt v(t)$  across the junction with  $v(t) = \frac{\hbar}{2e} \frac{d\phi}{dt}$ .

We recast Eq. (1) into a novel form of the dynamical washboard potential model with nonequilibrium modulations of certain parameters,

$$I = \frac{\hbar}{2eR_n} \frac{d\phi}{dt} + J(t) \sin[\phi(t) - \zeta(t)] + S(t). \quad (2)$$

Due to the nonlocality-in-time of Eq. (1), the phase difference in time  $\phi(t) - \phi(t')$  causes the nonequilibrium modulations  $I_{s,n}^{\text{neq}}(t) \equiv \int_{-\infty}^t dt' \mathcal{K}_{s,n}(t-t') e^{i\frac{\phi(t)-\phi(t')}{2}}$ .  $J(t)$  and  $\zeta(t)$  are, respectively, amplitude and argument of the nonequilibrium modulations of the supercurrent  $I_s^{\text{neq}}(t)$ , while  $S(t)$  is the imaginary part of the quasiparticle current  $I_n^{\text{neq}}(t)$ . The reformulation into Eq. (2) enables us to develop a qualitative analysis using the mechanical analogue of the so-called phase particle in a tilted washboard potential  $\mathcal{U}(\phi, t) = [S(t) - I]\phi - J(t) \cos[\phi - \zeta(t)]$  and a quantitative analysis employing an iterative approach.

*Qualitative analysis.*—The mechanical analogue of Eq. (2) allows a qualitative analysis of  $\phi(t)$  without seeking the exact solution. When  $I_c > I$ , the dynamics becomes stationary with  $\phi(t) - \phi(t') = 0$  converging to the fixed point  $\phi_x = \arcsin(I/I_c)$ . This results in  $V = 0$  and  $I_c = \int_0^\infty dt \mathcal{K}_s(t)$ . When  $I_c < I$ ,  $\phi(t)$  evolves in absence of a fixed point. Then, the phase difference in time modulates  $\mathcal{U}(\phi, t)$ . To analyze this complex behavior, we add factors  $e^{-t/t_m}$  to the memory kernels  $\mathcal{K}_{s,n}(t)$  by hand. These factors introduce a finite memory time  $t_m$ . We qualitatively analyze the influence of the past dynamics on  $\mathcal{U}(\phi, t)$  and  $\phi(t)$ , starting with an exactly solvable limit  $t_m \rightarrow 0$  (no memory). Subsequently, we turn on the nonlocality-in-time by increasing  $t_m$ . In the end, this gives rise to a qualitative understanding of the  $I$ - $V$  characteristics when  $I_c < I$ .

The limit  $t_m \rightarrow 0$  yields the RSJ model where Eq. (2) becomes local-in-time and exactly solvable:

$\phi(t) \rightarrow \phi_0(t) = 2 \arctan[\frac{I_c}{I} + \frac{\sqrt{I^2 - I_c^2}}{I} \tan \frac{eR_n t \sqrt{I^2 - I_c^2}}{\hbar}]$  and  $\mathcal{U}(\phi, t) \rightarrow \mathcal{U}_0(\phi) = -I\phi - I_c \cos \phi$  with  $J_0(t) = I_c$  and  $\zeta_0(t) = S_0(t) = 0$ , yielding the  $I$ - $V$  characteristics  $V = R_n \sqrt{I^2 - I_c^2}$ . In the low voltage regime  $V \ll I_c R_n$ ,  $\phi_0(t)$  shows an abrupt phase winding by  $2\pi$  for every period as a step-wise jump, generating sharp voltage pulses with  $\max\{v(t)\} \sim I_c R_n$  and time width  $\delta T \sim \hbar/(eI_c R_n)$ .

Next, we consider the memory effect with finite  $t_m < T$  and analyze the behavior of the tilted washboard potential  $\mathcal{U}(\phi, t)$ . We begin this analysis for pedagogical reasons by focusing on a single voltage pulse of  $\phi_0(t)$  appearing at  $t = 0$  with a short time width  $\delta T \ll T$ . Then, sufficiently long after or before the voltage pulse,  $\mathcal{U}(\phi, t)$  hardly varies from  $\mathcal{U}_0(\phi)$  owing to the finite memory time  $t_m$  and causality. However, in the vicinity of the voltage pulse  $0 < t < t_m$ , we argue that the abrupt  $2\pi$  phase winding modulates  $\mathcal{U}(\phi, t)$  with  $I_{s,n}^{\text{neq}}(t) \approx \int_{-\infty}^0 dt' \mathcal{K}_{s,n}(t-t') e^{\frac{t'-t}{t_m}} - \int_0^t dt' \mathcal{K}_{s,n}(t-t') e^{\frac{t'-t}{t_m}}$  using the expression below Eq. (2) [30]. The nonequilibrium modulations of  $\mathcal{U}(\phi, t)$  are determined by the memory kernels  $\mathcal{K}_{n,s}(t)$  via  $J(t) \approx I_c - 2 \int_t^{t+t_m} dt' \mathcal{K}_s(t') e^{-t'/t_m}$ ,  $\zeta(t) \approx \mathcal{K}_s(t) e^{-t/t_m} \delta T / I_c$ , and  $S(t) \approx -\mathcal{K}_n(t) e^{-t/t_m} \delta T$ . Hence,  $\mathcal{U}(\phi, t)$  oscillates around  $\mathcal{U}_0(\phi)$ . We compare our estimation of  $J(t)$  with exact numerical calculations for a tunnel junction coupling two BCS superconductors in Fig. 1. For this type of junction,  $\mathcal{K}_{n,s}(t)$  sinusoidally oscillate with the time scale  $\hbar/(2\Delta)$  due to energy-time uncertainty, and  $\mathcal{K}_{n,s}(t) \rightarrow 0$  for  $t \rightarrow \infty$  due to causality [31].

We can derive the general behavior of  $\phi(t)$  from the mechanical analogue of a phase particle in presence of a finite memory time  $t_m < T$ . According to the modulation of  $\mathcal{U}(\phi, t)$  around  $\mathcal{U}_0(\phi)$ , the phase particle exhibits back-and-forth motion. This can be described by an additional function  $\delta\phi(t)$ , which oscillates around zero. After sev-

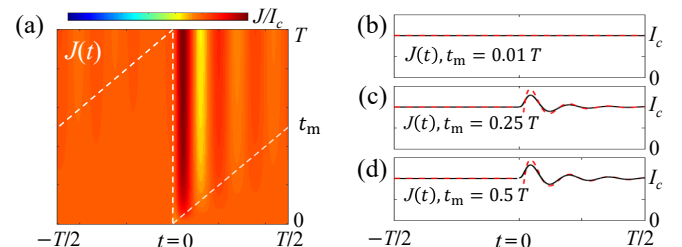


FIG. 1. Analytical estimation and numerical calculation of the modulating height  $J(t)$  of the dynamical washboard potential  $\mathcal{U}(\phi, t)$ . We depict a numerically calculated color map of  $J(t)$  with respect to the memory time  $t_m$  in (a). The time ranges where the voltage pulse modulates  $\mathcal{U}(\phi, t)$  are indicated as a guide for the eye (dashed lines). In the right panels, we present plots of  $J(t)$  for several  $t_m$  for a better comparison of analytics (dashed lines) to numerics (solid lines). The height  $J(t)$  of  $\mathcal{U}(\phi, t)$  oscillates around  $I_c$ . We use  $\phi_0(t)$  exhibiting  $\delta T/T = 0.05$  and the memory kernels from Ref. [31]. Note that  $\mathcal{U}(\phi, t + T) = \mathcal{U}(\phi, t)$  and  $\phi(t + T) = \phi(t) + 2\pi$  [32].

eral back-and-forth motions, the phase particle  $\phi(t)$  eventually advances by  $2\pi$  due to the lack of a fixed point for  $I_c < I$ . We replace  $\phi(t) \rightarrow \phi_0(t) + \delta\phi(t)$  including a memory effect. As we increase the nonlocality-in-time further  $T < t_m$ , more voltage pulses in the past contribute to the modulation of  $\mathcal{U}(\phi, t)$ .

We develop the following picture of the memory effect on the  $I$ - $V$  characteristics:  $I$  corresponds to the tilting of the dynamical washboard potential and  $V$  to the inverse of the time period  $T = \pi\hbar/(eV)$  satisfying  $\phi(t+T) = \phi(t) + 2\pi$ . Let us assume that a static washboard potential  $\mathcal{U}_0(\phi)$  should be tilted by  $I_0$  in order to generate a voltage drop  $V = \pi\hbar/(eT)$ . Then, the memory effect demands larger tilting  $I$  of the dynamical washboard potential  $\mathcal{U}(\phi, t)$  than  $I_0$ , since the memory effect makes it more difficult for the phase particle to advance by  $2\pi$  because of the back-and-forth motion. Hence, the memory effect changes the  $I$ - $V$  characteristics, accordingly.

*Quantitative analysis.*—We now present an analytical approach for the DC current-biased  $I$ - $V$  characteristics of a generic Josephson tunnel junction. The task is to calculate the DC current-bias  $I$  generating the DC voltage drop  $V$ . We approach this task by an iterative solution of Eq. (2). The  $N$ -th iteration step begins with calculating the dynamical modulations of  $\mathcal{U}_N(\phi, t)$  using the previous iterative solution  $\phi_{N-1}(t)$  with the period  $T = \pi\hbar/(eV)$ . The  $N$ -th iterative solution  $\phi_N(t)$  is obtained by solving Eq. (2) with  $\mathcal{U}_N(\phi, t)$ . Those iterations are repeated until the solution converges. Intriguingly, our quantitative analysis shows that the first iteration step is sufficient to obtain the  $I$ - $V$  characteristics to a good accuracy.

The reason for the power of the first iteration step is related to a clever choice of the initial ansatz  $\phi_0(t) = 2\arctan[\frac{I_c R_n + V \tan(eVt/\hbar)}{\sqrt{(I_c R_n)^2 + V^2}}]$ , inspired by the functional form of the solution of the RSJ model. Updating  $J_0(t) = I_c$ ,  $\zeta_0(t) = S_0(t) = 0$  into the dynamical modulations  $J_1(t)$ ,  $\zeta_1(t)$ ,  $S_1(t)$  by inserting  $\phi_0(t)$  into the expressions defined below Eq. (2), we take the memory effect into account. The first iterative solution  $\phi_1(t)$  is obtained from

$$I = \frac{\hbar}{2eR_n} \frac{d\phi_1}{dt} + J_1(t) \sin[\phi_1(t) - \zeta_1(t)] + S_1(t). \quad (3)$$

$\phi_1(t)$  exhibits back-and-forth motion with the correction  $\delta\phi_1(t) = \phi_1(t) - \phi_0(t)$ . We reduce Eq. (3) into the equation of motion of  $\delta\phi_1(t)$  in the regime  $J_1(t)/I_c - 1, \zeta_1(t), S_1(t)/I_c \ll 1$ . This implies that  $\mathcal{U}_1(\phi, t)$  oscillates weakly around  $\mathcal{U}_0(\phi)$ . The reduced equation of motion describes the dynamics of  $\delta\phi_1(t)$  in a different washboard potential with the height  $I_c$  but dynamically tilted by  $[I_c - J_1(t)] \sin \phi_0(t) - S_1(t)$ . Since the tilting is much smaller than its height,  $\delta\phi(t)$  lacks the  $2\pi$  phase winding and shows weak oscillations around zero with a small DC component. The iteration steps can be repeated, but the corrections due to additional small oscillations are negli-

gible.

This motivates us to use the first iteration to calculate the DC current-bias  $I$  generating the DC voltage drop  $V$  and analyze how well it works. We put  $\phi(t) = \phi_0(t) + \delta\phi(t)$  with a small oscillating correction  $\delta\phi(t)$  into Eq. (2), letting  $\phi(t)$  and  $\phi_0(t)$  share the period  $T = \pi\hbar/(eV)$  producing the DC voltage drop  $V$  with  $\delta\phi(t+T) = \delta\phi(t)$ . Collecting terms containing other than  $\phi_0(t)$  as  $\mathcal{O}[\delta\phi(t)]$ , we rewrite Eq. (2) as

$$I = \frac{\hbar}{2eR_n} \frac{d\phi_0}{dt} + J_1(t) \sin[\phi_0(t) - \zeta_1(t)] + S_1(t) + \mathcal{O}[\delta\phi(t)]. \quad (4)$$

To evaluate the DC current-bias  $I$ , we take the time-average of Eq. (4) over the period  $T = \pi\hbar/(eV)$ . Then, the time integral of  $\mathcal{O}[\delta\phi(t)]$  contains an integrand multiplied by  $\delta\phi(t)$ . Using  $\delta\phi(t+T) = \delta\phi(t)$ , we find  $\int_0^T dt f(t)\delta\phi(t) \lesssim \frac{A_m}{2m\pi} \int_0^T dt f(t)$ , where  $m$  and  $A_m$  are, respectively, the number of back-and-forth motions within a period and the amplitude of  $\delta\phi(t)$ . Since  $A_m$  is small and  $m > 1$ , we find that the time-average of  $\mathcal{O}[\delta\phi(t)]$  becomes negligibly smaller than  $I_c$ . Thus, we obtain this equation for the  $I$ - $V$  characteristics

$$I \approx \frac{V}{R_n} + \overline{J_1(t) \sin[\phi_0(t) - \zeta_1(t)] + S_1(t)}, \quad (5)$$

where  $\overline{f(t)} \equiv \frac{1}{T} \int_0^T dt f(t)$ .

Focusing on the low-voltage regime  $V < I_c R_n$ , by which we can approximate  $\phi_0(t)$ , we evaluate the time-averages in Eq. (5) further. This yields an analytical formula for the DC current-biased  $I$ - $V$  characteristics of Josephson tunnel junctions with generic memory kernels,

$$I \approx \sqrt{I_c^2 + \left(\frac{V}{R_n}\right)^2} + \frac{\hbar}{eI_c R_n} \sum_{n=0}^{\infty} (-1)^n \overline{\mathcal{K}_n\left(t + n \frac{\pi\hbar}{eV}\right)} - 2 \sum_{n=0}^{\infty} (-1)^n \int_{-\infty}^{-n \frac{\pi\hbar}{eV}} dt' \overline{\mathcal{K}_s(t-t')}. \quad (6)$$

This equation is the first main result of our work. The additional contributions of the second and third terms in Eq. (6) stem from the memory effects of the quasiparticle current and supercurrent at the current bias. Since memory kernels contain the retarded dynamics of electric fields from voltage pulses, the time-averaged memory kernels are the central physical quantities determining the  $I$ - $V$  characteristics at low voltages. The summations signify the influence of each voltage pulse in the past on the dynamical washboard potential. We discuss the opposite limit, i.e., the  $I$ - $V$  characteristics of Josephson tunnel junctions in the high-voltage regime  $I_c R_n < V$ , in the Supplemental Material by employing Eq. (5) [33].

*Werthamer equation with smeared DOS.*—We exemplify the validity of the analytical formula, Eq. (6), by looking at a concrete example of a Josephson tunnel junction. The junction consists of two BCS superconductors with a small junction cross section. The Werthamer

equation describes the Josephson effect by taking into account the memory kernels of the junction in Eq. (1). It shows good agreement with experiments, when smearing of the superconducting gap is considered [17, 34]. The smearing appears in realistic situations due to various mechanisms [34–39]. Considering the smeared DOS, we derive an analytical formula of the  $I$ - $V$  characteristics and compare it to numerics [15–17]. We show below that different types of the  $I$ - $V$  characteristics are interpolated within our theoretical framework as the smearing increases.

$$\frac{I}{I_c} \approx \sqrt{1 + \left(\frac{V}{I_c R_n}\right)^2} - \frac{4V}{\pi^2 V_g} + \frac{4 \arctan\left(\frac{\sin \frac{\pi V_g}{V}}{e^{\pi \gamma V_g/V} + \cos \frac{\pi V_g}{V}}\right)}{\pi^2(1 + \gamma^2)[K(-\gamma^2)]^2} \frac{V^2}{V_g^2} - \frac{4 \log \sqrt{2e^{-\frac{\pi \gamma V_g}{V}} \left(\cosh \frac{\pi \gamma V_g}{V} + \cos \frac{\pi V_g}{V}\right)}}{\pi^2(1 + \gamma^2)K(-\gamma^2)} \frac{V^2}{V_g^2}, \quad (7)$$

where  $\gamma = \Gamma/(2\Delta)$  and  $V_g = 2\Delta/e$ . The critical current  $I_c = \Delta/(eR_n)K(-\gamma^2)$  decreases as the smearing energy increases.  $K(x)$  is the complete elliptic integral of the first kind. We note that the last two terms on the right hand side in Eq. (7) stem from the retarded responses to voltage pulses in the past. The third term corresponds to the step-wise increasing quasiparticle current by photon-assisted tunneling [15]. The fourth term describes the subharmonic peaks of the supercurrent by self-coupling [4, 15].

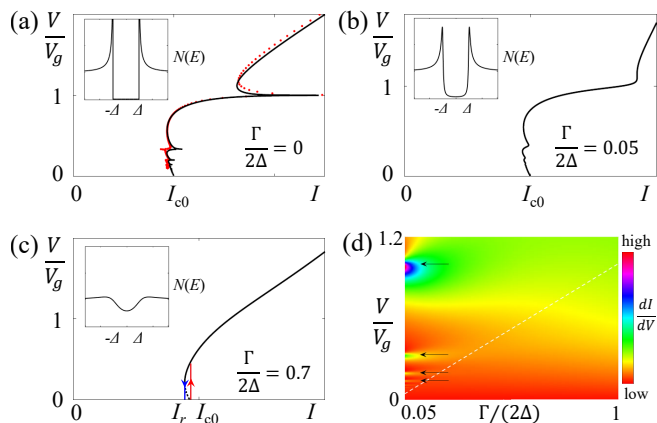


FIG. 2. DC current-biased  $I$ - $V$  characteristics based on the Werthamer equation with smeared DOS  $N(E)$ . In (a), our analytical result (solid line) is provided together with a numerical calculation (red dots) using Eq. (1) without smearing. Analytical calculations for  $\Gamma \ll \Delta$  and  $\Gamma \sim \Delta$  are shown in (b) and (c), respectively. The voltage staircases become visible as peaks in the colormap of  $dI/dV$  in (d).  $V/V_g = 1, 1/3, 1/5, 1/7$  are indicated with arrows from top to bottom.  $V = \Gamma/e$  is drawn as a guide to the eye (dashed line) and  $I_{c0} = \pi\Delta/(2eR_n)$ . Insets: Quasiparticle DOS  $N(E)$  corresponding to the chosen  $\Gamma$  in each panel [33].

We take into account the smeared DOS with an energy broadening  $\Gamma$  to describe BCS superconductors. This gives rise to memory kernels  $\mathcal{K}_s(t) = -\pi\Delta^2 e^{-\Gamma t/\hbar} J_0(t\Delta/\hbar) Y_0(t\Delta/\hbar)/(\hbar e R_n)$  and  $\mathcal{K}_n(t) = \pi\Delta^2 e^{-\Gamma t/\hbar} J_1(t\Delta/\hbar) Y_1(t\Delta/\hbar)/(\hbar e R_n)$  at zero temperature.  $J_n$  and  $Y_n$  are Bessel functions of first and second kinds, respectively. Symmetric superconducting gaps  $\Delta$  are considered for both superconductors for simplicity. Putting the above memory kernels into Eq. (6), we derive the DC current-biased  $I$ - $V$  characteristics in the low-voltage regime in analytical form, which is the second main result of our work,

We begin with the case without smearing, which has been studied extensively with numerical approaches [15, 16]. When  $\Gamma = 0$ , Eq. (7) reproduces the logarithmic divergence in the subharmonics at voltages  $V_p = V_g/(2p - 1)$  ( $p = 1, 2, \dots$ ) and  $I_c R_n = \pi\Delta/(2e)$  [4, 15]. We compare the analytical formula with numerics in Fig. 2(a). Along with the notable agreement in both calculations, our analytical approach clarifies that the logarithmic divergence stems from the infinitely large number of voltage pulses due to the algebraically decaying memory kernels  $\mathcal{K}_{n,s}(t) \sim 1/t$  for  $\Gamma = 0$ . This behavior suggests that the logarithmic divergence is washed out and limited by a finite measurement time in experiments.

For small smearing  $\Gamma \ll \Delta$ , Eq. (7) implies the emergence of voltage staircases in the absence of AC current bias, reported in recent experiments with high-quality Josephson junctions [20–24]. Notably, it is theoretically suggested that the dynamics of a qubit in junctions can replace the role of the AC current bias employing the quantum RSJ model [26, 27]. However, our theoretical analysis shows that voltage staircases can even appear in absence of both AC current bias and qubit dynamics in the junction. We discover that the feedback effect modulates the washboard potential dynamically with  $[S(t) - I]\phi - J(t) \cos[\phi - \zeta(t)]$ . This feedback effect becomes most significant when voltage pulses add constructively  $V_p = V_g/(2p - 1)$  ( $p = 1, 2, \dots$ ). The resulting dynamical modulation causes a similar behavior found in the quantum RSJ model with qubit dynamics [25–27]. Then, the phase particle is trapped against increased tilting by a current bias, which results in rather flat voltage drops at  $V_p$  [see Figs. 2(b) and 2(d)].

Moreover, the comparison of the time scales of memory kernels provides further understanding, for instance, related to its oscillation period  $T_\Delta = \hbar/(2\Delta)$  and decay-

ing time scale  $T_\Gamma = \hbar/\Gamma$ . The exponential decay with  $T_\Gamma = \hbar/\Gamma$  explains the absence of the logarithmic divergence occurring for  $\Gamma = 0$ . The decaying time  $T_\Gamma$  competes with the period of voltage pulses  $T = \pi\hbar/(eV)$ , as less contributions from the past add together at present with increasing period  $T$  between voltage pulses for a given  $T_\Gamma$ . Consequently, the voltage staircases appear approximately in the range  $\Gamma/e < V < 2\Delta/e$  [see Fig. 2(d)].

Finally, we consider the regime of large smearing  $2\Delta \lesssim \Gamma$ , at which the memory kernel shows over-damped oscillations. Then, the contributions from retarded responses, the last two terms in Eq. (7), become vanishingly small, and the  $I$ - $V$  characteristics at zero temperature qualitatively coincides with the one from the RSJ model [Fig. 2(c)]. However, we find that the nonequilibrium Josephson effect causes additional hystereses in the  $I$ - $V$  characteristics. Eq. (7) yields the recapturing current  $I_r = I_c\sqrt{1 - 4[K(-\gamma^2)]^2/\pi^4}$  where the voltage drop vanishes at backward current bias. The hysteresis emerges as our theory can capture the quasiparticle excitations and stored Josephson energy.

*Summary*—We provide a generic theory of the DC current-biased  $I$ - $V$  characteristics applicable to various types of Josephson tunnel junctions. In our theory, the information of the junction is contained in memory kernels. We derive an analytical formula which can be used as a powerful fitting function to experiments under appropriate conditions. In sharp contrast to the voltage-biased case, where multiple Andreev reflections of quasiparticles are responsible for subharmonics, we show that the supercurrent can play a major role in the DC current-biased  $I$ - $V$  characteristics. Our analytical formula can be employed to quantitatively evaluate the shape of the superconducting gap. It also explains the hystereses experimentally observed in low-dimensional Josephson junctions where the geometric capacitance is negligibly small.

This work was supported by the Würzburg-Dresden Cluster of Excellence on Complexity and Topology in Quantum Matter (EXC2147, project-id 390858490) and by the DFG (SPP1666 and SFB1170 “ToCoTronics”).

---

\* sang-jun.choi@physik.uni-wuerzburg.de

- [1] M. H. Cohen, L. M. Falicov, J. C. Phillips, Superconductive tunneling. *Phys. Rev. Lett.* **8**, 316 (1962).
- [2] B. D. Josephson, Possible new effects in superconducting tunneling, *Phys. Lett.* **1**, 251 (1962).
- [3] V. Ambegakokar and A. Baratoff, *Phys. Rev. Lett.* **10**, 486 (1963).
- [4] N. R. Werthamer, Nonlinear self-coupling of Josephson radiation in superconducting tunnel junctions, *Phys. Rev.* **147**, 255 (1966).
- [5] A. I. Larkin and Y. N. Ovchinnikov, Tunnel effect between superconductors in an alternating field, *Zh. Eksp. Teor. Fiz.* **51**, 1535 [*Sov. Phys. JETP* **24**, 1035 (1967)].
- [6] T. M. Kalpwijk, G. E. Blonder, and M. Tinkham, Explanation of subharmonic energy gap structure in superconducting contacts, *Physica (Amsterdam)* **109-110B+C**, 1657 (1982).
- [7] E. N. Bratus, V. S. Shumeiko, and G. Wendin, Theory of subharmonic gap structure in superconducting mesoscopic tunnel contacts, *Phys. Rev. Lett.* **74**, 2110 (1995).
- [8] D. Averin and A. Bardas, ac Josephson effect in a single quantum channel, *Phys. Rev. Lett.* **75**, 1831 (1995).
- [9] A. V. Zaitsev and D. V. Averin, Theory of ac Josephson effect in superconducting constrictions, *Phys. Rev. Lett.* **80**, 3602 (1998).
- [10] Y. Naveh and D. V. Averin, Nonequilibrium current noise in mesoscopic disordered superconductor–normal-metal–superconductor junctions, *Phys. Rev. Lett.* **82**, 4090 (1999).
- [11] D. E. McCumber, Effect of ac Impedance on dc voltage-current characteristics of superconductor weak-Link junctions *J. Appl. Phys.* **39**, 3113 (1968).
- [12] W. C. Stewart, Current-voltage characteristics of Josephson junctions, *Appl. Phys. Lett.* **12**, 277 (1968).
- [13] W. C. Scott, Hysteresis in the dc switching characteristics of Josephson junctions, *Appl. Phys. Lett.* **17**, 166 (1970).
- [14] W. A. Schlup, Adiabatic and pendulum approximations to the retarded Josephson equation, *J. Appl. Phys.* **49**, 3011 (1978).
- [15] D. G. McDonald, E. G. Johnson, R. E. Harris, Modeling Josephson junctions. *Phys. Rev. B* **13**, 1028 (1976).
- [16] W. A. Schlup, Solution of the Werthamer equation at finite temperatures, *Phys. Rev. B* **18**, 6132 (1978).
- [17] A. B. Zorin, K. K. Likharev, S. I. Turovets, Dynamics of Josephson tunnel junctions with a finite-width Riedel peak. *IEEE Trans. Magn.* **19**, 629 (1983).
- [18] W. A. Schlup, Investigation of the validity of generalizations of the adiabatic Josephson equation for a local junction by asymptotic expansions, *SQUID-Superconducting Quantum Interference Devices and their Applications* (De Gruyter, 1977).
- [19] S. H. Strogatz, *Nonlinear Dynamics and Chaos* (Addison-Wesley, New York, 1994), p.96.
- [20] O. Gül, *et al.* Hard superconducting gap in InSb nanowires, *Nano letters* **17**, 2690 (2017).
- [21] S. Charpentier, *et al.* Induced unconventional superconductivity on the surface states of Bi<sub>2</sub>Te<sub>3</sub> topological insulator, *Nature communications* **8**, 1 (2017).
- [22] W. Mayer, J. Yuan, K. S. Wickramasinghe, T. Nguyen, M. C. Dartiaillh, and J. Shabani, Superconducting proximity effect in epitaxial Al-InAs heterostructures. *Appl. Phys. Lett.* **114**, 103104 (2019).
- [23] J. Ridderbos, M. Brauns, A. Li, E. P. Bakkers, A. Brinkman, W. G. Van Der Wiel, and F. A. Zwanenburg, Multiple Andreev reflections and Shapiro steps in a Ge-Si nanowire Josephson junction, *Phys. Rev. Materials*, **3**, 084803 (2019).
- [24] P. Perla, *et al.* Fully in situ Nb/InAs-nanowire Josephson junctions by selective-area growth and shadow evaporation. *Nanoscale Advances* **3**, 1413 (2021).
- [25] J.-J. Feng, Z. Huang, Z. Wang, and Q. Niu, Hysteresis from nonlinear dynamics of Majorana modes in topological Josephson junctions, *Phys. Rev. B* **98**, 134515(R) (2018).
- [26] S.-J. Choi, A. Calzona, and B. Trauzettel, Majorana-induced DC Shapiro steps in topological Josephson junctions, *Phys. Rev. B* **102**, 140501(R) (2020).
- [27] D. O. Oriekhov, Y. Cheipesh, and C. W. J. Beenakker,

- Voltage staircase in a current-biased quantum-dot Josephson junction, Phys. Rev. B **103**, 094518 (2021).
- [28] A. Barone and G. Paterno, *Physics and applications of the Josephson effect*, (Wiley, New York, 1982), p. 30.
- [29] F. Tafuri, *Fundamentals and frontiers of the Josephson effect*, (Springer, Berlin, 2019).
- [30] The  $2\pi$  phase winding has flipped the sign of the second term and resulted in the additional modulation  $-2 \int_0^t dt' \mathcal{K}_{n,s}(t-t') e^{\frac{t'-t}{\tau_m}}$ , compared to the case without the phase winding.
- [31] R. E. Harris, Intrinsic response time of a Josephson tunnel junction, Phys. Rev. B **13**, 3818 (1976).
- [32] C. Zurbrugg, Periodic solutions of a pendulum-like integrodifferential equation with infinite retardation describing Josephson tunneling, Z. Angew. Math. Mech. **71**, 21 (1991).
- [33] See the Supplemental Material at (URL), which includes Refs. [5, 14, 40, 41], for the analytical formula of the DC current-biased  $I$ - $V$  characteristics at high voltages  $I_c R_n < V$ , and the derivation of the quasiparticle DOS with smearing energy  $\Gamma$ .
- [34] K. K. Likharev, *Dynamics of Josephson junctions and circuits*, (Gordon and Breach, New York, 1986).
- [35] V. Mourik, K. Zuo, S. M. Frolov, S. Plissard, E. A. Bakkers, and L. Kouwenhoven, Science **336**, 1003 (2012).
- [36] A. Das, Y. Ronen, Y. Most, Y. Oreg, M. Heiblum, and H. Shtrikman, Nat. Phys. **8**, 887 (2012).
- [37] M. T. Deng, C. L. Yu, G. Y. Huang, M. Larsson, P. Caroff, and H. Q. Xu, Nano Lett. **12**, 6414 (2012).
- [38] A. D. K. Finck, D. J. Van Harlingen, P. K. Mohseni, K. Jung, and X. Li, Phys. Rev. Lett. **110**, 126406 (2013).
- [39] A. B. Zorin, I. O. Kulik, K. K. Likharev, and J. R. Schrieffer, The sign of the interference current component in superconducting tunnel junctions, Sov. J. Low Temp. Phys. **5**, 537 (1979).
- [40] R. C. Dynes, V. Narayanamurti, and J. P. Garno, Direct measurement of a quasiparticle-lifetime broadening in a strong-coupled superconductor, Phys. Rev. Lett. **41**, 1509 (1978).
- [41] R. C. Dynes, J. P. Garno, G. B. Hertel, and T. P. Orlando, Tunneling study of superconductivity near the metal-insulator transition, Phys. Rev. Lett. **53**, 2437 (1984).

## Supplemental Material: Microscopic theory of the current-voltage characteristics of Josephson tunnel junctions

### DC CURRENT-BIASED $I$ - $V$ CHARACTERISTICS IN THE HIGH-VOLTAGE REGIME $I_c R_n < V$

We provide the  $I$ - $V$  characteristics of generic Josephson tunnel junctions in the high-voltage regime  $I_c R_n < V$ . We find that the ansatz in the main text can be written in the high-voltage regime as

$$\phi_0(t) = 2 \arctan \left[ \frac{I_c R_n + V \tan(eVt/\hbar)}{\sqrt{(I_c R_n)^2 + V^2}} \right] = \frac{2eV}{\hbar} t + 2 \frac{I_c R_n}{V} \cos^2 \left( \frac{eVt}{\hbar} \right) + \mathcal{O} \left[ \left( \frac{I_c R_n}{V} \right)^2 \right]. \quad (8)$$

By using  $\phi_0(t) \approx 2eVt/\hbar + 2(I_c R_n/V) \cos^2(eVt/\hbar)$  with the self-consistent equation Eq. (4) in the main text, we obtain the  $I$ - $V$  characteristics in the high-voltage regime  $I_c R_n < V$  for generic Josephson tunnel junctions,

$$I \approx \frac{V}{R_n} + \int_0^\infty d\tilde{t} \tilde{\mathcal{K}}_n(\tilde{t}) \sin \frac{eV\tilde{t}}{\hbar} + \frac{I_c R_n}{2V} \int_0^\infty d\tilde{t} \tilde{\mathcal{K}}_s(\tilde{t}) \cos \frac{eV\tilde{t}}{\hbar}. \quad (9)$$

The quasiparticle current, the first two terms, coincides with the  $I$ - $V$  characteristics of the DC voltage-biased case  $V$  due to the similarity of the dynamics of  $\phi_0(t)$  to that of the DC voltage-biased case  $\phi_0(t) = 2eVt/\hbar$ . However, the supercurrent shows the difference in the  $I$ - $V$  characteristics depending on the type of bias. Owing to the additional oscillating dynamics  $2(I_c R_n/V) \cos^2(eVt/\hbar)$  in case of the DC current bias, the supercurrent in the third term carries a non-vanishing DC component, which affects the  $I$ - $V$  characteristics. In contrast, the DC voltage-biased  $I$ - $V$  characteristics only include sinusoidal AC supercurrents.

Employing the memory kernels in the Werthamer equation without smearing energy  $\Gamma$ , we obtain the  $I$ - $V$  characteristics in the high-voltage regime,

$$I(V) \approx \frac{V + V_g}{R_n} E \left[ \left( \frac{V - V_g}{V + V_g} \right)^2 \right] - \frac{V_g(2V + V_g)}{R_n(V + V_g)} K \left[ \left( \frac{V - V_g}{V + V_g} \right)^2 \right] + I_c \frac{V_g^2}{4V^2} K \left( \frac{V_g^2}{V^2} \right), \quad (10)$$

where  $I_c R_n = \pi\Delta/(2e)$  for  $\Gamma = 0$ .  $K(x)$  and  $E(x)$  are the complete elliptic integrals of the first and second kind, respectively. Note that the DC supercurrent in the last term is responsible for the logarithmic divergence at  $V = V_g$ , which is absent in the DC voltage-biased  $I$ - $V$  characteristics. We use Eq. (10) for Fig. 2(a) in the main text.

## SMEARED DENSITY OF STATES OF BCS SUPERCONDUCTORS

We derive the density of states with the smearing parameter  $\Gamma$ . The density of states is calculated by

$$N(E) = -\frac{1}{\pi\mathcal{V}} \sum_{\mathbf{k}} \text{Im}\{G(\mathbf{k}, E + i\Gamma)\} = -\frac{1}{\pi\mathcal{V}} \sum_{\mathbf{k}} \text{Im} \left\{ \frac{E + i\Gamma + \xi_{\mathbf{k}}}{(E + i\Gamma)^2 - E_{\mathbf{k}}^2} \right\}. \quad (11)$$

We use the normal Green function of BCS superconductors  $G(\mathbf{k}, E + i\Gamma)$  with the smearing energy  $\Gamma$  added as an imaginary part to the energy.  $E_{\mathbf{k}} = \sqrt{\xi_{\mathbf{k}} + \Delta^2}$  is the single particle excitation spectrum of the Bogoliubov quasiparticles.  $\mathcal{V}$  is the volume of the system. By changing the summation over discrete wave numbers  $\mathbf{k}$  to an integration over the continuous energy  $\xi$ , the smeared density of states is calculated as

$$N(E) = N(0) \text{Re} \left\{ \frac{|E| - i\Gamma}{\sqrt{(|E| + i\Gamma)^2 - \Delta^2}} \right\}. \quad (12)$$

We note that the BCS DOS  $N(E) = N(0)\Theta(|E| - \Delta)|E|/\sqrt{E^2 - \Delta^2}$  is obtained in the limit  $\Gamma \rightarrow 0$ .  $\Theta(x)$  is the Heaviside step function. The smeared DOS  $N(E)$  is in good agreement with experimental measurements of the DOS using tunneling spectroscopy [40, 41].